SHARK-NIR waffle mode test report

Based on AO tests done in 2022-05-20

Prepared by Daniele Vassallo and Dino Mesa

Last modified on 2022-09-16

This report is aimed to discuss the results of the analysis of the data taken during the tests performed on 2022-05-20 using LUCI coupled with the M2 adaptive secondary mirror (ASM) of LBT. For the test two KL modes were adopted, namely modes #62 and #119, that were identified as promising in previous analysis using simulated data. Different turbulence was also applied to the data (no turbulence, seeing 0.55" and seeing 0.80"). Also different amplitudes were applied to the ASM ranging between 10 and 40 nm. All the data were taken with a simulated star and with an exposure time of 2.5 s. Each file was created with 10 DITs. Aside to the KL data, data with zero amplitude for the ASM were also taken in such a way that no spots were created in the image. Finally, also dark images were taken during the tests.

We grouped all the retrieved data in five different tests. The images of each test share the same characteristics. The five tests are the following:

1. **KL#62 with no turbulence**; in this case we retrieved 4 files with an amplitude of 20 nm and 5 files with zero amplitude (no spots in the image);
2. **KL#62 and a seeing of 0.55"**; in this case we retrieved 4 files with an amplitude of 20 nm and 3 files with zero amplitude (no spots in the image);
3. **KL#62 and a seeing 0.80"**; in this case we retrieved 4 files with an amplitude of 20 nm and 3 files with zero amplitude (no spots in the image);
4. **KL#119 and no turbulence**; in this case we retrieved 9 files with different amplitudes ranging between 10 and 40 nm. In any case only for five of these images we were able to identify clearly the spots. The other images were not used for the analysis. There is no correlation in this dataset between spots misidentification and amplitude of the KL.
5. **KL#119 and a seeing of 0.55"**; in this case we retrieved 13 images with different amplitudes ranging between 5 and 40 nm (for the case with 5 nm the spots were not visible). We also retrieved two files with zero amplitude (no spots in the image).

Data reduction: For the data reduction we selected for each file with visible spots the nearest (in time) file without any spots (zero amplitude). For the case of the test #4, where no file with zero amplitude was retrieved, we used to this aim the file with an amplitude of 10 nm for which it was not possible to identify any spot. We then adopted a python script that performed the following steps:

- For both the files (with and without the satellite spots) we subtracted a dark frame;
- We then subtracted the image without spots from the image with the spots. In such a way the noise in the resulting image was greatly reduced and each single spot was strongly highlighted;
- The central part of the image was masked to avoid that the central simulated star disturbs the detection of the symmetric spots;
- We then applied the python version of the FIND procedure. This procedure was generally able to retrieve large part of the spots, as can be seen in the two examples shown in Figure 1 and in Figure 2 where the red asterisks identify the positions of the spots found by the python procedure.

- We fitted a circle thorugh the positions of the retrieved spots. The center of the circle corresponds to the expected position of the star.
- As a check of the results, we excluded from the fit all the spots with a separation larger than the median separation plus the standard deviation or lower than the median separation minus the standard deviation (all these values are in pixels). We then fitted again a circle through the remaining values and verified that the final results did not change.

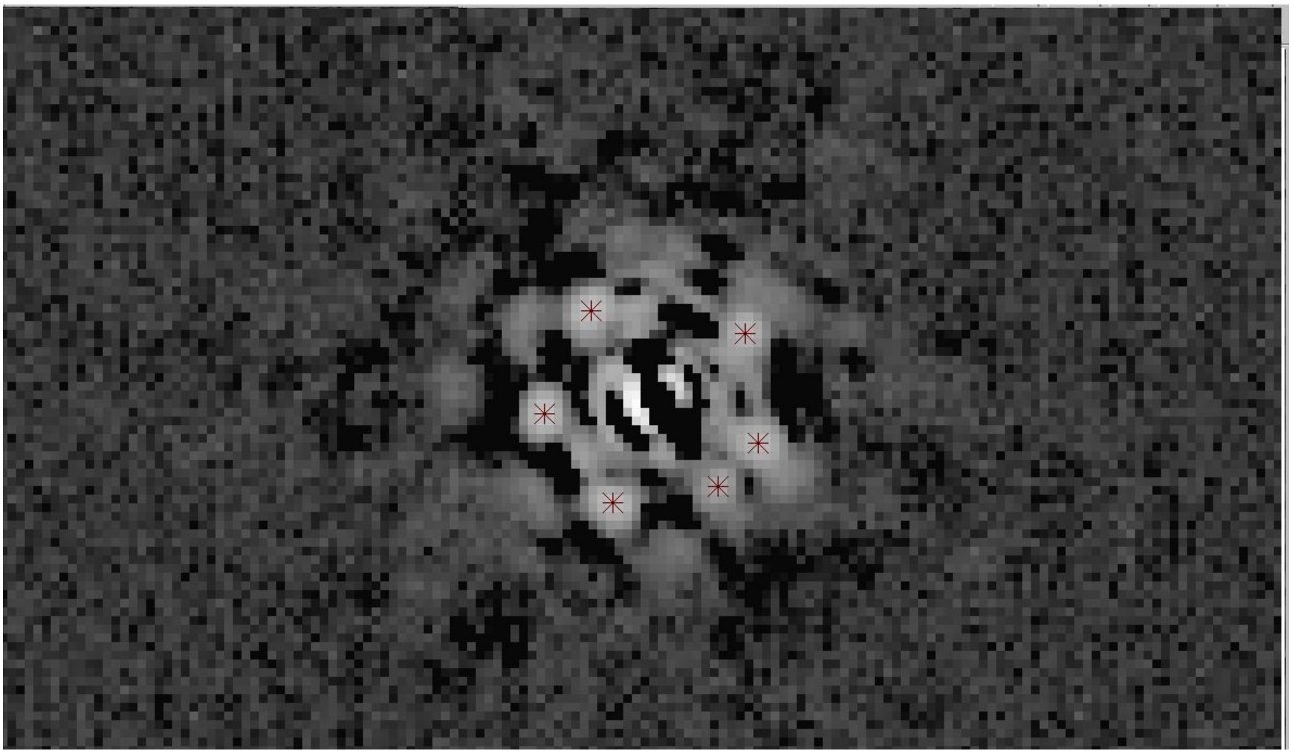

Figure 1 – Example of spots identification for one of the images obtained with KL#62.

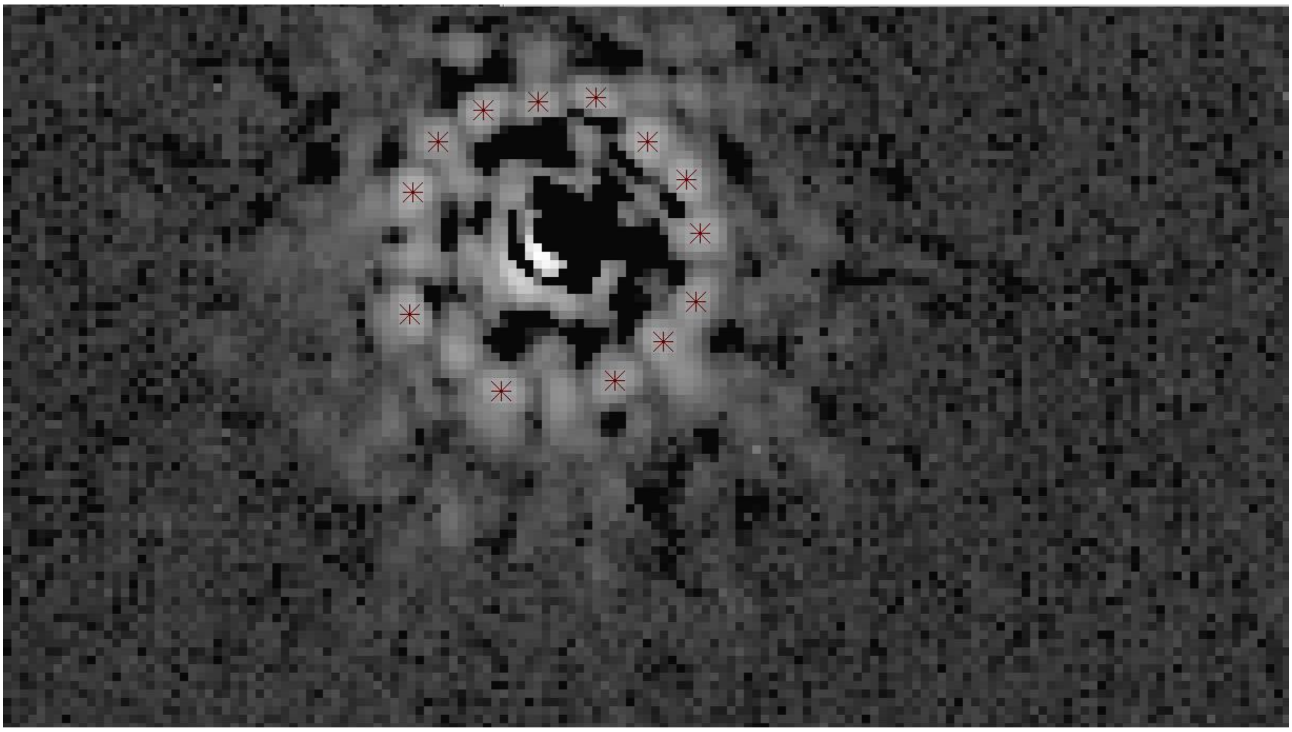

Figure 2 – Example of spots identification for one of the images obtained with KL#119.

As the PSF core is not physically masked, we are also able to measure directly its position and compare it to the center of the fitted circle. To compute the PSF core centroid we used a different python procedure that simply fits a 2D Gaussian to the PSF core. We stress here that this latter procedure will not be usable for SHARK during normal observation as the star will normally be behind the coronagraph.

Results:

Test #	X PSF			Y PSF			X circle			Y circle		
	Avg (pixel)	Std. dev. (pixel)	PtV (pixel)	Avg (pixel)	Std. dev. (pixel)	PtV (pixel)	Avg (pixel)	Std. dev. (pixel)	PtV (pixel)	Avg (pixel)	Std. dev. (pixel)	PtV (pixel)
1	835.128	0.085	0.181	1385.456	0.159	0.443	835.247	0.095	0.213	1385.437	0.178	0.426
1b	835.153	0.104	0.279	1385.432	0.129	0.307	///	///	///	///	///	///
2	848.195	0.021	0.044	1434.962	0.052	0.125	848.626	0.258	0.477	1434.656	0.186	0.360
2b	848.243	0.007	0.013	1435.116	0.010	0.019	///	///	///	///	///	///
3	883.191	0.119	0.279	1459.387	0.080	0.159	883.574	0.188	0.381	1459.315	0.288	0.610
3b	883.159	0.051	0.102	1459.464	0.022	0.043	///	///	///	///	///	///
4	791.104	0.030	0.090	1528.453	0.027	0.083	791.245	0.133	0.295	1528.254	0.136	0.306
4b	**No data**						///	///	///	///	///	///
5	835.416	0.069	0.221	1537.307	0.174	0.491	835.503	0.247	0.672	1537.000	0.186	0.330
5b	835.570	0.093	0.132	1537.518	0.075	0.106	///	///	///	///	///	///

Table 1 – Average position of the star in the five tests, measured both directly by fitting the PSF core (X PSF, Y PSF) and indirectly by using the symmetric spots method (X circle, Y circle). The PSF core position is measured twice, both using only the images with the KL on (first line) and using only the ones with the KL off (line b). We miss images with KL off for test#4.

In Table 1 we list the center position found in all the five tests described above, both measured directly using the PSF core (tagged with "PSF" in the Table) and indirectly using the symmetric spots (tagged with "circle" in the Table). Here we are giving the mean values obtained considering all the images retrieved for that particular test. For each measure we also report the corresponding standard deviation and peak to valley (PtV). Comparing the results obtained with the two methods, it is evident that the symmetric spots procedure is able to reproduce with good reliability the position of the center of the stellar PSF. We also are listing, in the list tagged with the letter 'b' after the number of the test, the position of the PSF center obtained considering the images for which no symmetric spot was introduced. This was done to check that the introduction of the symmetric spots is not changing the position of the PSF center. As can be seen by the comparison of the two lines from the same test, the position of the PSF is not changed in the two cases confirming that this is not an issue. During the test#4 no image without symmetric spots was taken so we cannot do any comparison in that case.

In Table 2 we list for each test the distance in pixels between the positions of the stellar center found using the two methods described above. As for the PSF core position, we used in this case the average of all the available images, without distinguishing between images with spots and images without. The maximum separation is just above 0.5 pixels and in general the distance is comparable with its error, meaning that the difference between methods is statistically not significant.

Test #	Distance (pixel)	Total error (pixel)
1	0.105	0.313
2	0.554	0.332
3	0.411	0.363
4	0.244	0.194
5	0.341	0.367

Table 2 - Distance in pixels between the center positions found using the two methods described above. In the third column, we report the error on the distance, computed as the square sum of individual X/Y standard deviations (columns 'Std. dev.' in Table 1).

Absolute positions difference significantly from one test to the other. In order to better visualize this, in Table 3 we subtracted the absolute positions of test#1 (columns "Avg") from the corresponding positions of the other tests. This allows us to understand whether these strong variations are induced by the KL or rather by variations in the test conditions not related to the KL (e.g. turbulence). Since the differences in the position of the circle center (ΔX circle, ΔY circle) match very well the ones of the PSF without KL, we can conclude that the KL is not responsible for such shifts.

Test #	ΔX PSF (pixel)	ΔX circle (pixel)	ΔY PSF (pixel)	ΔY circle (pixel)
2	13.067	13.379	49.506	49.219
3	48.063	48.327	73.931	73.878
4	-44.024	-44.002	142.997	142.817
5	0.288	0.256	151.851	151.563

Table 3 - Average position of the star in tests #2 to #5 relative to the corresponding position of the star in test#1.

We also tested the reproducibility of the position of individual spots in different images taken in the same conditions. In general, the observation with KL#62 allowed detecting between 6 and 8 spots while using KL#119 we were able to detect up to 15 spots. Some spots were faint and they were retrieved just in few cases. To perform our test we then used one bright spot for each test reporting, aside to its absolute position (that is changing for each test) both the standard deviation on the position (both X and Y) and the peak-to-valley distribution. These results are reported in Table 4. We then report in Table 5 the same results obtained for a faint spot (however visible for all the images of a test). While in the bright case we used the same spot for all the five steps, in the faint case the spot is changing from one test to the other.

Test #	X position			Y position		
	Avg (pixel)	Std. Dev. (pixel)	PtV (pixel)	Avg (pixel)	Std. Dev. (pixel)	PtV (pixel)
1	830.451	0.118	0.260	1373.441	0.181	0.430
2	843.411	0.048	0.108	1422.925	0.026	0.062
3	878.428	0.133	0.305	1447.352	0.059	0.132
4	785.155	0.043	0.099	1511.283	0.078	0.212
5	829.552	0.147	0.391	1519.981	0.070	0.210

Table 4 – Absolute position, standard deviation and peak-to-valley variation on the X and Y position of a bright spot for all the five tests.

	X position			Y position		
Test #	**Avg (pixel)**	**Std. Dev. (pixel)**	**PtV (pixel)**	**Avg (pixel)**	**Std. Dev. (pixel)**	**PtV (pixel)**
1	822.475	0.108	0.233	1383.773	0.172	0.409
2	846.498	0.041	0.096	1446.121	0.095	0.201
3	875.958	0.181	0.398	1469.550	0.109	0.206
4	783.121	0.170	0.413	1544.303	0.133	0.320
5	847.112	0.224	0.788	1549.532	0.100	0.354

Table 5 – Same as Table 4 but for a faint spot.

The results listed in Table 4 and in Table 5 demonstrate that the position of the spots is generally stable both for a brigth and for a faint spot. Similar results are obtained for other spots.

Conclusions:

The results described above allow to draw the following conclusions:

1. The procedure we have prepared is effectively able to detect the symmetric spots.
2. Fitting the spots with a circle allows to determine a reliable position of the stellar PSF center, as clearly shown in Table 3. This method is valid independetly from the criteria used to define the spots as demonstrated by the similar results obtained excluding some of the spots at larger or lower separation than the median value.
3. The differences in the absolute position of the circle center (ΔX circle, ΔY circle) from one test to the other match very well the ones of the PSF without KL, in a way that we can conclude that the KL mode is NOT responsible for such discrepancies. The changes in the absolute positions of the PSF and of the spots (represented by the circle center) from one test to the other are related instead to the variation of the injected turbulence.
4. The comparison between the position of the star measured using the spots and the one measured directly using the PSF core allows to conclude that this procedure is precise with uncertainties of the order of few tenths of pixel. Indeed, the maximum difference is of around 0.5 pixel PtV. The accuracy that is required should be of the order of minimum 1/10 of the best Inner Working Angle provided by the SHARK-NIR coronagraphs (2 λ/D with the FQPM), which corresponds to about 100µm on the scientific focal plane. This means that the required accuracy shall be of the order of 10 microns, corresponding to about half of the pixel size. Thus, the reported maximum difference of 0.5 pixels is indeed compatible with the required accuracy. Anyway, the expected higher precision of the SHARK-NIR instrument (due to the higher intrinsic Strehl) with respect to LUCI (used for these tests) will probably allow to obtain even better accuracies. Tests to be performed with SHARK-NIR when at the telescope will be needed to confirm this.
5. The single spots are retrieved with a precision of the order of 0.3-0.4 pixels PtV in different images. This will allow to use them as further indication of the accuracy of our method for the determination of the PSF stellar center, and it may also open to other tracking techniques which consider only a spot or a subset of them.
6. Additional test are required to assess the optimal KL modes amplitude allowing both to create bright spots and not saturating the AO WFS, although test#4 and #5 are giving already evidence that amplitudes <20nm cannot be used for our purposes. Test#4 also shows that in some cases even amplitudes of 20nm or bigger are not producing bright enough spots, but considering the rarity of this occurrences we are led to think that this might be due to something not optimized in the specific acquisition (e.g. NCPA removal or WFS gains).